Evaluating Wire Configurations for Tension Band Constructs using a Canine Greater Trochanteric Osteotomy Model

Running Head: Evaluating Tension Band Wire Configurations

Authors:
*Elizabeth Thompson,[1] DVM, Diplomate ACVS

*Amir K. Robe,[2] BS

Simon C. Roe,[1] BVSc, PhD, Diplomate ACVS

Jacqueline H. Cole,[2] PhD

*Thompson & Robe are considered equal first authors as they contributed equally to the study

[1] Department of Clinical Sciences, College of Veterinary Medicine, North Carolina State University, Raleigh, NC

[2] Joint Department of Biomedical Engineering, University of North Carolina, Chapel Hill, NC, and North Carolina State University, Raleigh, NC

The authors have no financial support to disclose.

The authors declare no conflict of interest related to this report.

Corresponding Author: Jacqueline H. Cole
Joint Department of Biomedical Engineering
University of North Carolina and North Carolina State University
911 Oval Drive
Campus Box 7115
Raleigh, NC 27695-7115
Tel: 919-515-5955
Fax: 919-513-3814
jacquecole@ncsu.edu

ABSTRACT

Objective: To investigate the stability of four tension band wiring configurations alone without the contributions of K-wire stabilization.

Study design: *ex vivo* experimental

Sample population: Sixty-four tension band wiring constructs

Methods: Four tension band configurations were applied to a metal trochanteric osteotomy model based on a canine femur: figure-of-eight with one twist (OT), figure-of-eight with two twists (TT), dual interlocking single loop (DISL), and double loop (DL). Configurations were mechanically tested under both monotonic loading (n = 8 per configuration) and incremental cyclic loading (n = 8 per configuration). Initial tension after tying, residual tension remaining after each cycle, and failure load at 2 mm of displacement (considered equivalent to clinical failure) were recorded.

Results: The initial tension and the load to 2 mm of displacement was lower for OT wires compared to TT wires. The DL was the strongest and most stable configuration, generating greater initial tension, maintaining a greater percentage of residual tension under incremental cyclic loads, and resisting higher load before failure at 2 mm. Failure load was highly correlated with initial tension.

Conclusion: This model enabled evaluation of tension band wire configuration independent of the fixation pin portion of the construct. Wire configurations that can be tightened to a greater tension during tying, like the DL, are better able to resist the tensile loads experienced by the construct.

Clinical impact: In clinical situations where high tensile loads are expected, a tighter, more secure tension band wire configuration may be warranted.

Keywords: tension band wire, fracture fixation, osteotomy, stabilization, load resistance

1. INTRODUCTION

The tension band (TB) technique has been in use since the 1970s as a method to resist distracting forces from a ligament or tendon on a bone fragment and convert those tensile forces into compression to help stabilize the fragment.[1-3] TB has been used for fixation in a variety of locations and clinical scenarios, including transpositions of the tibial tuberosity and osteotomies or fractures of the medial malleolus, distal fibula, greater trochanter, and olecranon.[4-9] The general approach involves securing the position of the bone fragment with two K-wires or pins (depending on the size of the fragment) and placing a figure-of-eight wire opposite the direction of pull of the attached ligament or tendon to prevent bending of the pins and maintain fragment position.

Complications with TB fixation are migration of the K-wires, osteomyelitis, nonunion or delayed union, implant breakage, comminution of the small bone fragment, and neuropraxia.[5,10] To reduce the rate of complications, the TB technique has been improved through several mechanical studies examining the impact of pin and wire diameter, type of wire configuration, and osteotomy plane. In a polymer model, larger pin diameter and thicker wire resulted in stronger constructs, and the figure-of-eight configuration was stronger than a single wire loop.[11,12] In an ulna osteotomy model, a double loop configuration resisted greater load at 2 mm of displacement compared to the standard figure-of-eight with two twists.[13] A dual interlocking single loop configuration resisted similar loads to the standard figure-of-eight constructs. This study also showed that the wire must be placed in contact with the pins and the bone fragment to prevent fragment displacement with low loads.

Previous TB studies have incorporated a variety of configurations in the presence of K-wires with or without other securing devices, such as lag screws or bone staples, to determine the most effective (i.e., strongest, most stable) wire construct.[11-22] However, the load resistance of the wire portion alone, without the confounding influence of K-wire stabilization, has not been evaluated and may inform improved TB wire designs to mitigate the persisting complications with TB fixation. While cerclage wires are known to resist higher loads before loosening when tied to greater tension,[23] the tension achieved with different tension band wire configurations is unknown. The objectives of this study were to examine 1) the amount of initial tension generated during tying for various TB configurations and 2) their ability to resist applied tensile loads before elongating to failure. We hypothesized that, compared with figure-of-eight configurations with one or two twists, dual interlocking single loop and double loop configurations would generate greater initial tension, resist greater load to 2 mm of displacement, and better retain residual tension with incremental cyclic loading. Additionally, we hypothesized that the load required to cause 2 mm of displacement (in a monotonic test) and the remaining residual tension after reaching 2 mm of displacement (in a cyclic test) would be positively correlated with the initial tension generated during tying the wire.

2. MATERIALS AND METHODS

2.1. Trochanteric Osteotomy Model

A trochanteric osteotomy model was designed to evaluate the load resistance of the wire portion of the construct independently, without contributions from the K-wires. An anatomically correct, solid brass “femur” was milled using a computer model created from a computed tomography scan of a normal right femur of a 30-kg canine. The solid femur model was modified to simulate a greater trochanteric osteotomy by cutting the trochanter fragment off the “bone” at an angle of 45 degrees to the long axis (Figure 1). Both cut surfaces were polished to minimize friction as the trochanter fragment moved proximally when loaded. Two 2.4-mm diameter 316LVM stainless steel pins were inserted perpendicular to the “osteotomy” line into the craniolateral and caudolateral aspects of the trochanter fragment. Because the pins were only in the trochanter fragment and did not extend across the osteotomy line into the rest of the “bone,” the trochanter fragment was only constrained by the wire configuration being assessed. To facilitate creation of the TB loops, the exposed pin tips were bent over, and a 2.5-mm diameter hole was drilled transversely through the distal aspect of the proximal metaphysis to serve as the distal anchor for the TB wire. This hole was positioned 12 mm distal to the distal edge of the osteotomy and 6 mm in from the lateral surface.

To test the TB constructs in the orientation of physiological loading, the femur model was rigidly fixed to a custom jig at an angle of 45° and secured in a servohydraulic load frame (858 Mini Bionix II, MTS Systems Corporation, Eden Prairie, MN) (Figure 1). To apply loads to the greater trochanter fragment a stainless steel eyebolt (#210 Everbuilt, Home Depot) was fitted at the fragment apex to mimic the attachment site of the gluteal tendon. The eyebolt link was connected to a steel chain (3410T74, 1225 kg load capacity, McMaster-Carr, Elmhurst, IL) using a D-Shackle (3824T71, McMaster-Carr). The top end of the chain was connected to a 15-kN load cell using another D-Shackle. The load cell was mounted to the linear actuator of the load frame. Prior to tying each specimen, the actuator was adjusted so that the trochanter fragment was in its anatomic position. To facilitate wire placement, the trochanter fragment was temporarily stabilized with a small pin that passed through the fragment into the parent "bone." Once the wire was positioned, and prior to tightening, the temporary pin was removed.

2.2 Tension Band Configurations

Four TB configurations were tested (Figure 2), including the figure-of-eight with one twist (OT), a figure-of-eight with two twists (TT), the dual interlocking single loop (DISL) construct, and a double loop (DL) construct modified from a previously published one.[13] All constructs were formed with 316L, 1.0-mm orthopaedic wire (18 gauge, IMEX Veterinary, Longview, TX). The OT configuration was formed by passing the wire through the distal anchor hole, crossing the lateral aspect of the femur model, wrapping around the pins, and connecting back to its other end with a twist knot (Figure 2A). The TT configuration was formed in a similar manner, except that a loop was formed in the wire that passed from the anchor hole to the pins (Figure 2B). This loop, and the joined wire ends, were twisted, resulting in both portions of the figure-of-eight being tightened.

The DISL configuration employed two wires, each with a 2-mm loop formed at one end (Figure 2C). The distal wire was passed through the distal anchor hole, and the loop was positioned adjacent to the hole on the cranial surface. The proximal wire was passed around the pins, with the loop beside the more cranial pin. The free end of the distal wire was passed across the lateral aspect of the femur model and through the loop of the proximal wire. The free end of the proximal wire was passed across the lateral aspect of the femur model and through the loop of the distal wire. The two free ends were introduced into a wire tightener (Item 391.21, DePuy Synthes Vet, West Chester, PA) and secured to the cranks. The cranks were turned simultaneously to tighten the wires until the operator deemed appropriate tightness had been reached. While holding that tension, the wire tightener was twisted to lock the ends to each other.

The DL configuration was formed from a length of wire with a 2-mm loop formed at its midpoint (Figure 2D). This loop was positioned between the pins and the free ends passed around the pins, crossed over the lateral aspect of the femur model, passed through the distal anchor hole, and bought back, and through, the loop. The ends were introduced into a wire tightener, secured to the cranks, and the wires tightened simultaneously until the operator deemed appropriate tightness had been obtained. While maintaining crank tension, the wire tightener was bent over. The cranks were turned in reverse to release 1 cm of wire, which was bent flat and then cut.

2.3 Mechanical Testing

For each test, the trochanter fragment was moved to a “reduced” position and secured with the temporary pin, and the load cell output was set to zero. The wire constructs were positioned, but not tightened, and the temporary pin was removed. The wire configurations were then tightened and the knots completed. To examine the effectiveness of the twist-and-lay technique used for the OT and TT constructs, the tension generated during the tying process (*tying tension*) was recorded for these two configurations prior to completing the final folding or setting of the knot. The *initial tension* was recorded as the initial force after tying was complete but before additional loads were applied.

Monotonic tests were performed on one set of wires (n=8 per configuration) by distraction to failure at an actuator speed of 50 mm/min. Time, force, and displacement data were recorded at 100 Hz (TestStar™ IIs, version 3.5C, MTS Systems Corp.). The mechanism by which the wire elongated was noted from direct observation and video recordings of the tests. All data processing was performed using MATLAB® (The MathWorks, Inc., Natick, MA). Force-displacement curves were generated, and the *failure load* was determined as the force measured at 2 mm of displacement, which was considered to be the equivalent of clinical failure for this study.

Cyclic tests were performed on a second set of wires (n=8 per configuration) using an incrementally increasing loading protocol to evaluate loosening.[23] Each construct was distracted at an actuator speed of 50 mm/min for one cycle at each load level. The first applied load was 50 N, and the load was increased incrementally by 25 N until the applied load at which 2 mm of displacement was reached, which was considered to be the equivalent of clinical failure. During each cycle, the constructs were distracted up to the desired load and then returned to the original "zero" position. Time, force, and displacement data were recorded at 50 Hz throughout testing. The following parameters were determined from the testing data: *residual tension* remaining in the wire at the end of each cycle, *failure load* at 2 mm of displacement, and *final residual tension*, measured as the force remaining at the end of the cycle where 2 mm of displacement was achieved.

2.4 Statistical Analyses

All statistical analyses were performed in SAS (SAS University Edition, SAS Institute Inc., Cary, NC) with a significance level of 0.05. For the monotonic loading data, twist-and-lay effectiveness was examined for the OT and TT figure-of-eight constructs by comparing differences in tying tension and initial tension using paired t-tests. Differences among the four configurations were examined for the initial tension and failure load at 2 mm of displacement using one-way ANOVAs (fixed factor = configuration) with Tukey adjustments for multiple comparisons. To account for heterogeneity of variances among configurations, the variance-weighted Welch's ANOVA was used.[24] The relationship between failure load and initial tension was determined with linear correlation analysis, and the Pearson correlation coefficient was calculated.

For the incremental cyclic loading data, configuration differences were assessed for the initial tension, failure load at 2 mm of displacement, and final residual tension using Welch's one-way ANOVAs (fixed factor = configuration) with Tukey adjustments for multiple comparisons. To compare the residual tension at the end of each cycle across configurations, a repeated measures analysis was performed using a generalized linear mixed model (procedure GLIMMIX) with one fixed factor (configuration), the repeated factor (cycle), and their interaction, with a modified Kenward-Roger approximation for the denominator degrees of freedom in the *F* tests.[25] In this model, the repeated factor (cycle) was treated as an R-side random effect, and the covariance matrix was modeled with a first-order autoregressive, first-order moving average structure (ARMA(1,1)). For each cycle, the residual tensions were compared between configurations using simple effect differences based on least squares means with Tukey-Kramer adjustments for multiple comparisons. The relationship between the final residual tension and initial tension was determined with linear correlation analysis, and the Pearson correlation coefficient was calculated.

3. RESULTS

During the monotonic tests, none of the wire configurations broke before 2 mm of displacement. By visual inspection, the DL initially underwent slight wire stretch prior to the two bent-over wires lifting up as load continued to be applied. The DISL initially elongated via stretching of each end loop. For both figure-of-eight constructs, after a brief period of initial stretch or flattening, elongation occurred by untwisting of the knot(s).

The twist-and-lay method of tying was effective for the TT configuration, increasing the tension by an average of 39% after bending over the twisted wire (42 ± 6 N tying tension vs. 56 ± 12 N initial tension, $p = 0.020$). The tension in the OT construct did not change significantly with the twist-and-lay method (33 ± 5 N vs. 36 ± 9 N, $p = 0.38$). Greater initial tension was generated with the DL configuration (128 ± 24 N) than the DISL (46 ± 5 N), TT (56 ± 12 N) and OT (36 ± 9 N) configurations ($p < 0.0001$ for all, Figure 3). The initial tension of the DISL was not significantly different than that of the TT or OT, but it was greater in the TT than in the OT ($p = 0.041$). The failure load at 2 mm of displacement was greater for the DL (402 ± 39 N) than the DISL (206 ± 14 N), TT (199 ± 20 N), and OT (165 ± 15 N) configurations ($p < 0.0001$ for all, Figure 4). The failure load of the DISL was not significantly different than that of the TT configuration, but both DISL and TT failure load was greater than that of the OT configuration ($p = 0.0092$ and 0.039, respectively). The failure load was linearly correlated with the initial tension (slope = 2.3 ± 0.15, $r = 0.945$, $p < 0.0001$).

For the incremental cyclic tests, the modes of failure were the same as described for the monotonic tests. For most cycles (50-250 N), the residual tension remaining at the end of the cycle was greater for DL than DISL, TT, and OT ($p < 0.05$), and it was only greater than DISL after the 275-N cycle (Figure 5). Residual tension was also greater in DISL than OT for cycles 75-150 N. By the end of the 11th cycle (300 N), all of the TT and OT and all but one of the DISL samples had reached the 2-mm failure point, but only one DL sample had failed, and the remaining DL samples maintained 19% of their initial tension. Similar to monotonic loading, the DL construct had higher failure loads at 2 mm (333 ± 48 N) than the DISL (247 ± 35 N, $p = 0.0003$), TT (229 ± 25 N, $p < 0.0001$), and OT (217 ± 30 N, $p < 0.0001$) constructs (Figure 6). At failure, which occurred at different cycles for each sample, the residual tension after the last cycle was significantly higher in the DL (11 ± 3 N) than in the DISL (1.0 ± 1.9 N), TT (2.7 ± 3.7 N), and OT (1.4 ± 3.5 N) configuration ($p < 0.0001$ for all, Figure 7). The final residual tension after reaching 2 mm was only greater than zero for DL and was not significantly different from zero for DISL, TT, and OT. The residual tension after the last cycle was linearly correlated with the initial tension before the first cycle (slope = 0.11 ± 0.019, $r = 0.736$, $p < 0.0001$).

4. DISCUSSION

As hypothesized, independent of K-wire stabilization, the double loop tension band wiring construct performed best of the four configurations tested, generating the greatest initial tension (2.3-3.5 times greater than the other configurations), resisting the highest load before 2 mm of displacement (2.0-2.4 times greater), and maintaining the greatest percentage of the initial tension under incremental cyclic loading. The failure load was highly correlated with and scaled with the initial tension by a factor of 2.3, so creating more tension in a TB construct during tying means that it will resist greater loads before it begins to loosen. Our results are consistent with previous studies, where the double loop generated greater static tension and a higher yield load[26] and resisted higher loads at 2 mm of displacement,[13] when compared to single loop or twist knots. In our study, the figure-of-eight TB construct with two twists resisted distraction of the fragment better than the one with one twist and thus was able to achieve a 21% higher force before failure at 2 mm (199 N vs. 165 N). Similarly, in a human cadaver study involving reduction of an olecranon osteotomy, the figure-of-eight TB wiring using two tightening knots was more effective in preventing motion under forces involved in active mobilization of the elbow immediately after operation compared to one with one twist.[14]

The greater initial tension with the DL results primarily from the use of a wire tightener to tighten the construct. The cranks enable the wire to be tensioned more effectively than other gripping instruments, and while some of that tension is lost as the arms are folded over, much is retained, resulting in the higher loads measured. The ability to resist load in these constructs relates to the mode by which the knots are "undone," with the twist styles untwisting and the arms of the loop styles unbending. With two arms, the DL configuration can better resist distraction, and higher loads must be applied before it loosens to the point of failure. Given that the knot or fold is the weak point of the system, this finding also suggests that more force is required to unbend two arms (DL) than to untwist two wires wrapped around each other as is present in the other three constructs. We found the following factors were important for producing the most secure construct and maximizing TB performance: 1) forming small loops to reduce the impact of loop elongation under load[13] (DL, DISL); 2) pressing the wire flat to the bone fragment and minimizing laxity as it is looped around; and 3) maintaining wire tension throughout tying, by applying continual pressure on wire tightener cranks while bending over the wire for DL[23] or pulling up during the twist-and-lay technique for OT and TT.

Contrary to our hypothesis, the DISL construct did not achieve a higher initial tension than the TT or OT constructs, although it did resist a higher monotonic load before 2 mm of displacement than OT, and it had a higher residual tension under cyclic loading than OT in the early cycles. Tightening the more complex DISL configuration is more difficult than the other configurations in this study, even with the use of the wire tightener, which may explain the inability to achieve a higher initial tension than with the figure-of-eight constructs. When loaded, the loops in the DISL elongated first, resulting in yield and elongation of the construct at lower loads. After this initial elongation, however, the configuration was stiffer and resisted higher loads, although this generally occurred after the clinical failure point of 2 mm displacement. Therefore, using clinically relevant criteria, the DISL construct was no more effective than the TT or OT constructs and was more difficult to form and tie.

One unique aspect of this study is the analysis of the tying process to help understand the differences between the different wire configurations in terms of the separate tightening and securing processes during tying. The twist-and-lay technique used for the figure-of-eight constructs was able to maintain (OT) or even increase by 39% (TT) the wire tension during the flattening process. After the twist was formed to a perceived tightness of just less than optimal, the knot was pulled up and an additional half twist was formed while simultaneously laying it over. The twist-and-lay technique is preferred over the technique of pushing the completed twist flat, which results in greater tension loss during the flattening process.[27] The greater increase in the construct with two twists likely occurred, because both loops of the figure-of-eight are individually tightened for an even tension distribution. For the one twist configuration, the single twist is not effective in tightening the loop that does not have a knot. The advantage of two twists is further supported by the higher initial tension and resistance to load before failure at 2 mm displacement compared to wires with just one twist.

The femur model and setup for testing the TB configurations in this study were designed to be anatomically correct and simulate a physiological loading direction on the greater trochanter during gait, yet also isolate the performance of the wiring portion of the construct and remove the contributions of K-wire stabilization and bone stiffness. In previous studies using bone models, the materials used to simulate bone were more compliant, such as Delrin® bar models or wooden patella models,[11,12,20,21] introducing compliance within the testing structure that could potentially confound the mechanical property measurements of the constructs alone. Similar to our study, some previous studies used anatomical loading, but they inserted K-wires across the fracture gap for stability and thus did not isolate the performance of the wiring configurations under loading.[11-14,16,18-22,28,29] Other studies isolated the wiring configurations but did not perform anatomical loading.[23,30-33] To our knowledge our study is the first to incorporate all of these aspects, providing an isolated comparison of various tension band wiring configurations without contributions from other parts of the stabilization system.

In conclusion, our greater trochanteric osteotomy model, without K-wires bridging the "fracture" gap, provided an effective means for isolating the performance of different tension band wiring configurations. Testing all wires on the same "bone" allowed for direct comparisons among the different configurations. The double loop was the best configuration in this study, primarily due to its substantially higher initial tension, which conferred the greatest resistance to load compared with the other three configurations. The two twist figure-of-eight was superior in initial tension and load resistance than the one twist figure-of-eight and thus should still be considered if a tensioning device is not available to aid in tying the double loop configuration or if space within the surgical field is inadequate to accommodate it. This study evaluated the behavior of the wire configurations during tying, with a single load to failure (as might occur with an inadvertent overexertion by a patient), and with different magnitudes of repeated loading. Future work could examine the fatigue properties under low-load cyclic loading, which may provide insight into the *in vivo* performance of these constructs. While the current study used a canine femur model to evaluate tension band wiring, determining the strongest configuration to resist applied loads is important, regardless of the species or anatomical location. This study helps elucidate stronger configurations to dictate appropriate surgical decision-making when a fracture or osteotomy requires fixation in a location where large tensile forces are applied to a fragment.

REFERENCES

1. Weber BG, Vasey H. [Osteosynthesis in Olecranon Fractures]. *Z Unfallmed Berufskr*. 1963; 56: 90-96.
2. Wolfgang G, Burke F, Bush D, et al. Surgical treatment of displaced olecranon fractures by tension band wiring technique. *Clin Orthop Relat Res*. 1987: 192-204.
3. Denny HR. The use of the wire tension band in the treatment of fractures in the dog. *J Small Anim Pract*. 1975; 16: 173-183.
4. Gibbons SE, Macias C, Tonzing MA, Pinchbeck GL, McKee WM. Patellar luxation in 70 large breed dogs. *J Small Anim Pract*. 2006; 47: 3-9.
5. Halling KB, Lewis DD, Cross AR, Kerwin SC, Smith BA, Kubilis PS. Complication rate and factors affecting outcome of olecranon osteotomies repaired with pin and tension-band fixation in dogs. *Can Vet J*. 2002; 43: 528-534.
6. Hauptman J, Butler HC. Effect of Osteotomy of the Greater Trochanter with Tension Band Fixation on Femoral Conformation in Beagle Dogs. *Veterinary Surgery*. 1979; 8: 13-18.
7. Ostrum RF, Litsky AS. Tension band fixation of medial malleolus fractures. *J Orthop Trauma*. 1992; 6: 464-468.
8. Palmer RH, Aron DN, Chambers JN. A combined tension band and lag screw technique for fixation of olecranon osteotomies. *Vet Surg*. 1988; 17: 328-332.
9. Parkinson DE, Joseph R, Edelman R. Biomechanical principles of tension band wiring applied to fractures of the distal fibula and fifth metatarsal base. *J Foot Surg*. 1988; 27: 149-156.

10. Macko D, Szabo RM. Complications of tension-band wiring of olecranon fractures. *J Bone Joint Surg Am*. 1985; 67: 1396-1401.

11. Neat B, Kowaleski MP, Litsky AS, Boudrieau RJ. The effects of wire diameter and an additional lateral wire on pin and tension-band fixation subjected to cyclic loads. *Vet Comp Orthop Traumatol*. 2006; 19: 213-218.

12. Neat BC, Kowaleski MP, Litsky AS, Boudrieau RJ. Mechanical evaluation of pin and tension-band wire factors in an olecranon osteotomy model. *Vet Surg*. 2006; 35: 398-405.

13. Grafinger MS, Roe SC, Spodnick G, Smith ES. Biomechanical comparison of dual interlocking single loop and double loop tension band techniques to the classic AO tension band technique for repair of olecranon osteotomies in dogs. *Vet Surg*. 2007; 36: 141-148.

14. Fyfe IS, Mossad MM, Holdsworth BJ. Methods of fixation of olecranon fractures. An experimental mechanical study. *J Bone Joint Surg Br*. 1985; 67: 367-372.

15. Halling KB, Lewis DD, Cross AR, Sammy RJ, Rapoff AJ. Biomechanical comparison of a circular external skeletal fixator construct to pin and tension band wire fixation for the stabilization of olecranon osteotomies in dogs: a cadaveric study. *Vet Surg*. 2003; 32: 324-335.

16. Hutchinson DT, Horwitz DS, Ha G, Thomas CW, Bachus KN. Cyclic loading of olecranon fracture fixation constructs. *J Bone Joint Surg Am*. 2003; 85-A: 831-837.

17. Mullett JH, Shannon F, Noel J, Lawlor G, Lee TC, O'Rourke SK. K-wire position in tension band wiring of the olecranon - a comparison of two techniques. *Injury*. 2000; 31: 427-431.

18. Reising K, Konstantinidis L, Helwig P, Wagner FC, Sudkamp NP, Strohm PC. Biomechanical testing of an innovative fixation procedure to stabilize olecranon osteotomy. *Proc Inst Mech Eng H*. 2014; 228: 1146-1153.
19. Wu CC, Tai CL, Shih CH. Biomechanical comparison for different configurations of tension band wiring techniques in treating an olecranon fracture. *J Trauma*. 2000; 48: 1063-1067.
20. Ali M, Kuiper J, John J. Biomechanical analysis of tension band wiring (TBW) of transverse fractures of patella. *Chin J Traumatol*. 2016; 19: 255-258.
21. John J, Wagner WW, Kuiper JH. Tension-band wiring of transverse fractures of patella. The effect of site of wire twists and orientation of stainless steel wire loop: a biomechanical investigation. *Int Orthop*. 2007; 31: 703-707.
22. Kozin SH, Berglund LJ, Cooney WP, Morrey BF, An KN. Biomechanical analysis of tension band fixation for olecranon fracture treatment. *J Shoulder Elbow Surg*. 1996; 5: 442-448.
23. Roe SC. Mechanical characteristics and comparisons of cerclage wires: introduction of the double-wrap and loop/twist tying methods. *Vet Surg*. 1997; 26: 310-316.
24. Welch BL. On the Comparison of Several Mean Values - an Alternative Approach. *Biometrika*. 1951; 38: 330-336.
25. Kenward MG, Roger JH. An improved approximation to the precision of fixed effects from restricted maximum likelihood. *Computational Statistics & Data Analysis*. 2009; 53: 2583-2595.
26. Blass CE, Piermattei DL, Withrow SJ, Scott RJ. Static and Dynamic Cerclage Wire Analysis. *Veterinary Surgery*. 1986; 15: 181-184.

27. Wähnert D, Lenz M, Schlegel U, Perren S, Windolf M. Cerclage handling for improved fracture treatment. A biomechanical study on the twisting procedure. *Acta Chir Orthop Traumatol Cech*. 2011; 78: 208-214.
28. Gruszka D, Arand C, Nowak T, Dietz SO, Wagner D, Rommens P. Olecranon tension plating or olecranon tension band wiring? A comparative biomechanical study. *Int Orthop*. 2015; 39: 955-960.
29. Parent S, Wedemeyer M, Mahar AT, et al. Displaced olecranon fractures in children: a biomechanical analysis of fixation methods. *J Pediatr Orthop*. 2008; 28: 147-151.
30. Bostrom MP, Asnis SE, Ernberg JJ, et al. Fatigue testing of cerclage stainless steel wire fixation. *J Orthop Trauma*. 1994; 8: 422-428.
31. Lenz M, Perren SM, Richards RG, et al. Biomechanical performance of different cable and wire cerclage configurations. *Int Orthop*. 2013; 37: 125-130.
32. Meyer DC, Ramseier LE, Lajtai G, Notzli H. A new method for cerclage wire fixation to maximal pre-tension with minimal elongation to failure. *Clin Biomech (Bristol, Avon)*. 2003; 18: 975-980.
33. Schultz RS, Boger JW, Dunn HK. Strength of stainless steel surgical wire in various fixation modes. *Clin Orthop Relat Res*. 1985: 304-307.

FIGURE LEGENDS

Figure 1. Solid brass right femur model with a 45° osteotomy (arrow), rigidly mounted in a custom jig for mechanical testing of tension band configurations. Loads were applied via a steel chain at an angle of 45° to mimic gluteal tendon loading.

Figure 2. Tension band wiring configurations on the right femur model with a 45° osteotomy: A) Figure-of-eight with one twist (OT), B) figure-of-eight with two twists (TT), C) dual interlocking single loop (DISL), and D) double loop (DL). The DISL construct was formed with two wires (I – distal wire, II – proximal wire).

Figure 3. Initial tension for the four tension band configurations. Mean ± standard deviation. **p < 0.0001 for DL vs. DISL, TT, and OT. *p = 0.041 for TT vs. OT.

Figure 4. Monotonic test. Failure load at 2 mm of displacement for the four tension band configurations. Mean ± standard deviation. **p < 0.0001 for DL vs. DISL, TT, and OT. *p = 0.0092 for DISL vs. OT and p = 0.039 for TT vs. OT.

Figure 5. Cyclic test. Residual tension after each incremental loading cycle for the four tension band configurations. Least squares mean ± 95% confidence interval at each cycle until failure. Multiple comparisons between configurations at each cycle made using Tukey-Kramer adjustments: *p < 0.05 for DL vs. DISL, TT, and OT. #p < 0.05 for DL vs. DISL only. †p < 0.05 for DISL vs. OT.

Figure 6. Cyclic test. Failure load at 2 mm of displacement for the four tension band configurations. Mean ± standard deviation. **$p = 0.0003$ for DL vs. DISL and $p < 0.0001$ for DL vs. TT and OT.

Figure 7. Cyclic test. Final residual tension (after failure at 2 mm was reached) for the four tension band configurations. Mean ± standard deviation. **$p < 0.0001$ for DL vs. DISL, TT, and OT.

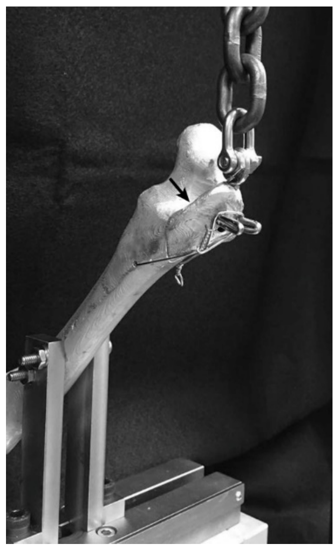

Figure 1. Solid brass right femur model with a 45° osteotomy (arrow), rigidly mounted in a custom jig for mechanical testing of tension band configurations. Loads were applied via a steel chain at an angle of 45° to mimic gluteal tendon loading.

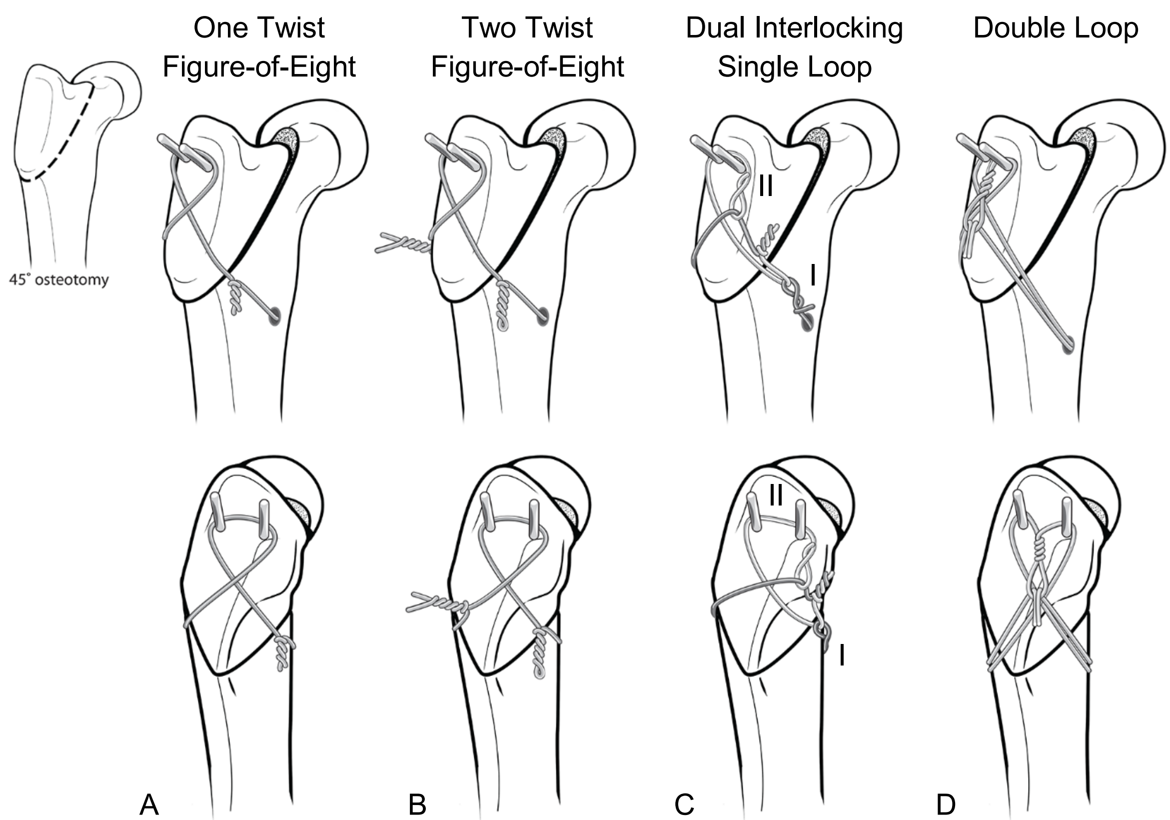

Figure 2. Tension band wiring configurations on the right femur model with a 45°osteotomy: A) Figure-of-eight with one twist (OT), B) figure-of-eight with two twists (TT), C) dual interlocking single loop (DISL), and D) double loop (DL). The DISL construct was formed with two wires (I – distal wire, II – proximal wire).

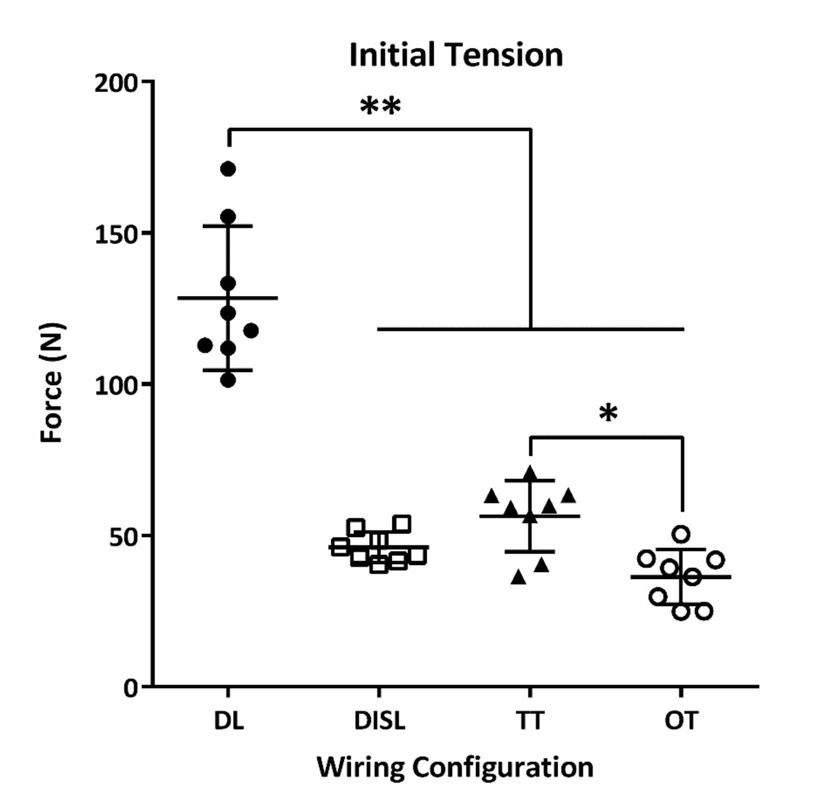

Figure 3. Initial tension for the four tension band configurations. Mean ± standard deviation. **p < 0.0001 for DL vs. DISL, TT, and OT. *p = 0.041 for TT vs. OT.

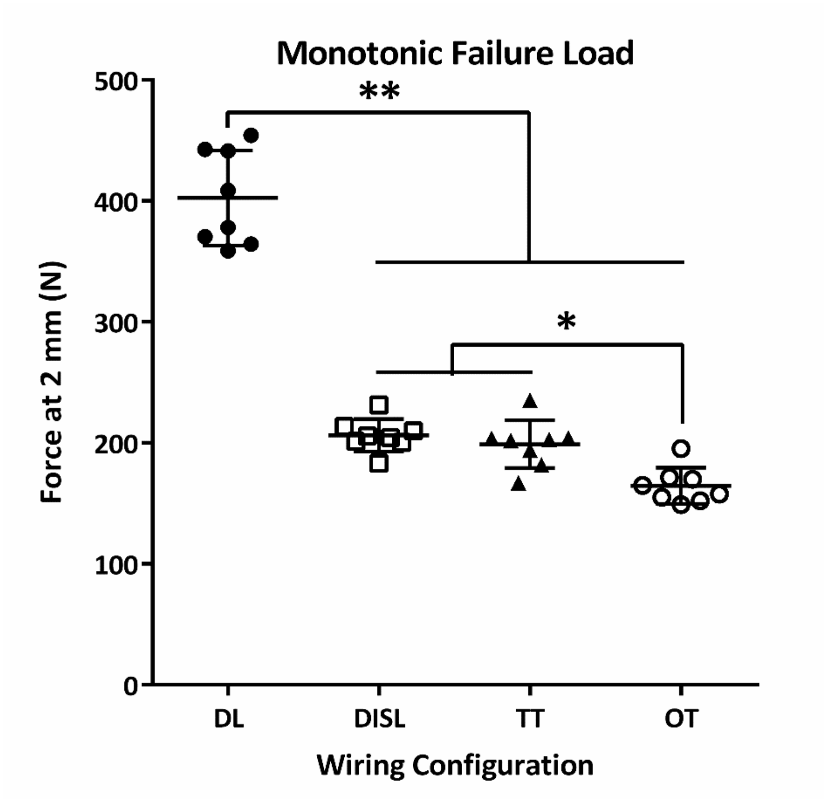

Figure 4. Monotonic test. Failure load at 2 mm of displacement for the four tension band configurations. Mean ± standard deviation. **p < 0.0001 for DL vs. DISL, TT, and OT. *p = 0.0092 for DISL vs. OT and p = 0.039 for TT vs. OT.

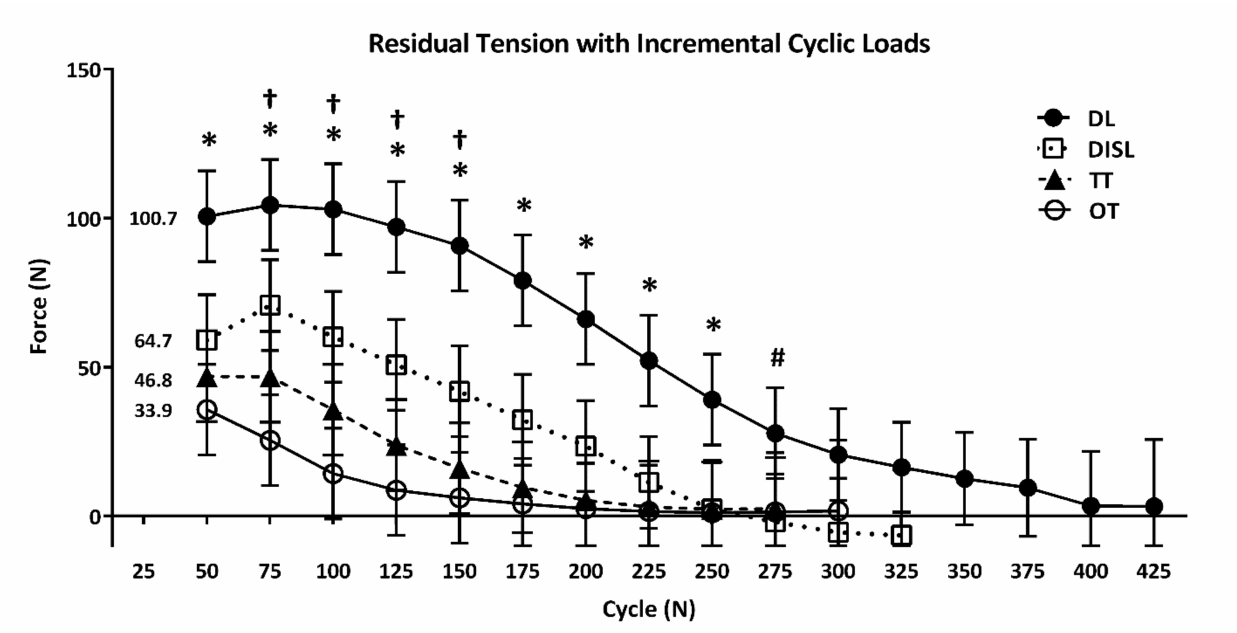

Figure 5. Cyclic test. Residual tension after each incremental loading cycle for the four tension band configurations. Least squares mean ± 95% confidence interval at each cycle until failure. Multiple comparisons between configurations at each cycle made using Tukey-Kramer adjustments: *$p < 0.05$ for DL vs. DISL, TT, and OT. $^{\#}p < 0.05$ for DL vs. DISL only. $^{\dagger}p < 0.05$ for DISL vs. OT.

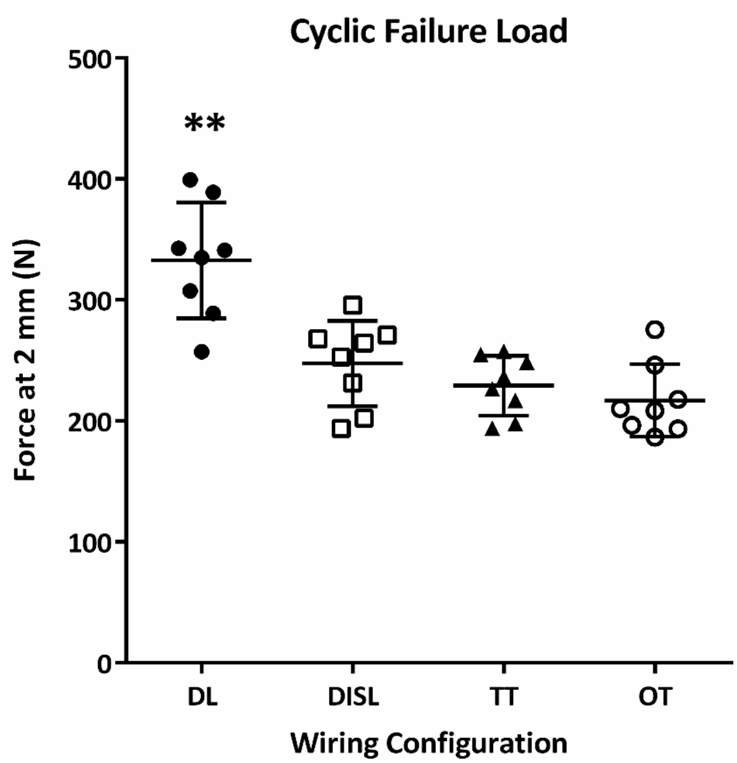

Figure 6. Cyclic test. Failure load at 2 mm of displacement for the four tension band configurations. Mean ± standard deviation. **$p = 0.0003$ for DL vs. DISL and $p < 0.0001$ for DL vs. TT and OT.

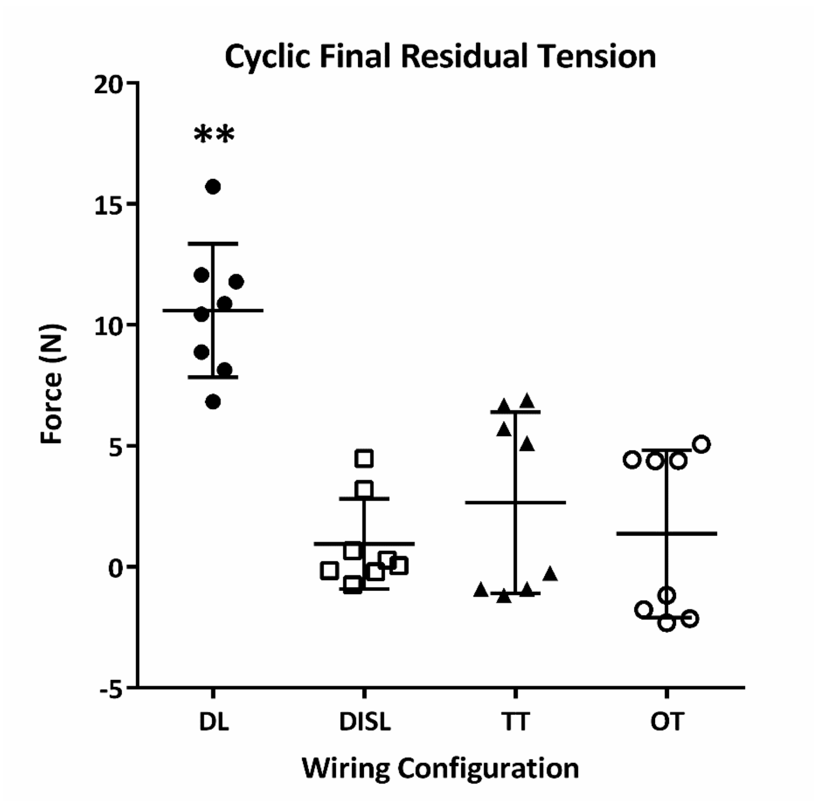

Figure 7. Cyclic test. Final residual tension (after failure at 2 mm was reached) for the four tension band configurations. Mean ± standard deviation. **$p < 0.0001$ for DL vs. DISL, TT, and OT.